Draft version April 23, 2021
Typeset using LaTeX **twocolumn** style in AASTeX63



# Prospects for detecting gravitational waves from eccentric sub-solar mass compact binaries

Yi-Fan Wang (王一帆)[1,2] and Alexander H. Nitz[1,2]

[1] *Max-Planck-Institut für Gravitationsphysik (Albert-Einstein-Institut), D-30167 Hannover, Germany*
[2] *Leibniz Universität Hannover, D-30167 Hannover, Germany*

## ABSTRACT

Sub-solar mass black hole binaries, due to their light mass, would have to be primordial in origin instead of the result of stellar evolution. Soon after formation in the early Universe, primordial black holes can form binaries after decoupling from the cosmic expansion. Alternatively, primordial black holes as dark matter could also form binaries in the late Universe due to dynamical encounters and gravitational-wave braking. A significant feature for this channel is the possibility that some sources retain non-zero eccentricity in the LIGO/Virgo band. Assuming all dark matter is primordial black holes with a delta function mass distribution, $1M_\odot - 1M_\odot$ binaries formed in this late Universe channel can be detected by Advanced LIGO and Virgo with at their design sensitivities with a rate of $\mathcal{O}(1)$/year, where 12%(3%) events have eccentricity at gravitational-wave frequency 10 Hz, $e^{10\mathrm{Hz}} \geq 0.01(0.1)$, and non-detection can constrain the binary formation rate within this model. Third generation detectors would be expected to detect sub-solar mass eccentric binaries as light as $0.01M_\odot$ within this channel, if they accounted for the majority of the dark matter. Furthermore, we use simulated gravitational-wave data to study the ability to search for eccentric gravitational-wave signals using quasi-circular waveform template bank with Advanced LIGO design sensitivity. Assuming binaries with a delta function mass of $0.1(1)M_\odot$ and the eccentricity distribution derived from this late Universe formation channel, for a match-filtering targeted search, 41%(6%) of the signals would be missed compared to ideal detection rate due to the mismatch in the gravitational-wave signal from eccentricity.

*Keywords:* Gravitational Waves — Eccentricity — Primordial Black Holes

## 1. INTRODUCTION

Gravitational-wave astronomy has gradually evolved into a routine window for observing compact binaries comprising black holes and/or neutron stars. Up to now, over fifty gravitational wave events have been identified by Advanced LIGO (Aasi et al. 2015) and Virgo (Acernese et al. 2015), all from compact binary coalescences (Abbott et al. 2020; Nitz et al. 2019). These detections have had significant astrophysical implications, including inferring stellar population properties (The LIGO Scientific Collaboration et al. 2020a), testing the validity of general relativity (The LIGO Scientific Collaboration et al. 2020b), and determining the value of the Hubble constant (Abbott et al. 2017).

In addition to routine detection, gravitational-wave data analysis is also searching for exotic objects from hypothesis, such as primordial black holes (Abbott et al. 2018a, 2019; Nitz & Wang 2021). Primordial black holes are hypothesized to form by direct collapse in dense regions of the early Universe (Zel'dovich & Novikov 1967; Hawking 1971; Carr & Hawking 1974) and are consistent with the properties required for a candidate of cold dark matter (Carr & Kuhnel 2020). A variety of astrophysical observations including from gravitational lensing have searched for primordial black holes and placed upper limits on the abundance with their null results, which shows that primordial black holes with a single mass are not likely to account for all dark matter (e.g., Carr & Kuhnel (2020); Green & Kavanagh (2020) for recent reviews). Nevertheless, as gravitational wave astronomy opens a new channel to observe stellar mass black holes, we investigate the event rate and prospects for searching for gravitational waves emitted from binary primordial black holes in the LIGO/Virgo sensitive band ($\sim 10 - 1000$ Hz). In particular, we focus on sub-solar mass binary mergers with non-zero eccentricity.

Corresponding author: Yi-Fan Wang (王一帆)
yifan.wang@aei.mpg.de

There are two viable ways for primordial black holes to form binaries. In the early Universe, after their initial formation, a nearest pair of primordial black holes can form a binary if the gravitational attraction is strong enough to decouple from the cosmic expansion (Nakamura et al. 1997; Sasaki et al. 2016). To be detected by gravitational-wave detectors, the binaries would have had sufficient time to circularize their orbits, thus the gravitational wave signals are not expected to have eccentricity by the time they enter the LIGO and Virgo sensitive band. On the other hand, primordial black hole binaries may also form by dynamical capture due to gravitational-wave braking in the late Universe in dark matter halos. A significant feature for this formation channel is the retention of non-zero eccentricity in the LIGO/Virgo band if the binaries form at close separation. This latter scenario is the focus of this work.

Bird et al. (2016) has studied the event rate of GW150914-like, i.e., $30M_\odot$ binary black hole merger. Their results show that the event rate is consistent with the empirical rate estimated from GW150914 (Abbott et al. 2016a,b). However, it is challenging to confirm that GW150914 is indeed primordial in origin and not the result of stellar evolution, leaving the question still open. Cholis et al. (2016) has investigated the eccentricity distribution for $30M_\odot$ binaries in the late Universe scenario. Meanwhile, given conventional stellar evolution models, sub-solar mass ($\leq 1M_\odot$) compact binary coalescence can only be due to primordial black holes, instead of stellar products, because they are lighter than the minimum mass of neutron stars (Timmes et al. 1996; Suwa et al. 2018). Therefore, in this work we only consider the mass range $[0.01, 1]\ M_\odot$, which is a smoking gun for primordial black holes, extending the work of Bird et al. (2016); Cholis et al. (2016) to sub-solar mass region. Primordial black holes in this mass range are predicted by a variety of formation theories, e.g., early Universe QCD phase transition (Jedamzik 1997; Byrnes et al. 2018; Carr et al. 2021)

Assuming a delta function distribution of mass, we first estimate the event rate and eccentricity distribution of sub-solar mass primordial black hole binaries formed in dark matter halos in Section 2. The merger rate of sub-solar mass binaries is shown to be higher than that of $30M_\odot$ binary primordial black holes as considered in Bird et al. (2016) by one to two orders or magnitude. With design sensitivity, the Advanced LIGO and Virgo observatories would be expected to detect one $1M_\odot - 1M_\odot$ binary with eccentricity $e^{10\mathrm{Hz}} \geq 0.1$ at a gravitational-wave frequency of 10 Hz with $\sim 10$ years of observation, if the fraction of primordial black hole in dark matter is 100%. Third generation detectors would detect primordial black hole binaries with a single mass varying from $0.01M_\odot$ to $1M_\odot$ and eccentricity distribution derived from this late Universe formation channel. Non-detection in the future would put constraints on the event rate modeling. In Section 3, we investigate the capability of the current match-filtering search pipeline using a quasi-circular waveform template bank to identify signals with eccentricity by simulated gravitational wave data. Results show that 41% and 6% of the signals would be missed compared to the idealized maximum for $0.1M_\odot - 0.1M_\odot$ and $1M_\odot - 1M_\odot$ binaries, respectively, arising from the mismatch of gravitational wave signals from eccentricity. Section 4 presents the discussions and conclusions.

## 2. EVENT RATE AND ECCENTRICITY DISTRIBUTION

In this section we consider the event rate and eccentricity distribution of compact binaries formed in the late Universe through two body encounters for a delta function mass distribution which we allow to vary within $[0.01, 1]M_\odot$. More complex mechanisms may also induce eccentric binaries, such as three body interaction via Kozai-Lidov effects (Kozai 1962; Lidov 1962), but they are not considered in this work and investigations will be left for the future.

We briefly review the two body dynamics for primordial black hole binary formation following Maggiore (2008); Peters & Mathews (1963); Turner (1977); O'Leary et al. (2009); Bird et al. (2016); Cholis et al. (2016). Specifically, we derive the overall event rate for primordial black hole binary coalescence with component mass $M_{\rm PBH} = 0.01/0.1/1\ M_\odot$. To aid in comparison to other works in this field, we state our eccentricity distributions at a fiducial dominant-mode gravitational-wave frequency of 10 Hz, which is denoted by $e^{10\mathrm{Hz}}$.

Two black holes can form a binary in an encounter due to gravitational-wave emission. The binary formation criterion is that the released gravitational-wave energy $\delta E_{\rm GW}$ exceeds the two-body kinetic energy

$$\delta E_{\rm GW} \geq \frac{1}{2}\mu v_{\rm rel}^2, \tag{1}$$

where $\mu = m_1 m_2/(m_1 + m_2)$ is the reduced mass, $m_1$ and $m_2$ are the component masses of the binary, and $v_{\rm rel}$ is the relative velocity of two black holes. In this work we only consider equal mass primordial black hole binaries, therefore we set $m_1 = m_2 = M_{\rm PBH}$.

At Newtonian order, the released gravitational wave energy is (Peters & Mathews 1963; Turner 1977)

$$\delta E_{\rm GW} = \frac{8}{15}\frac{G^{7/2}}{c^5}\frac{(m_1+m_2)^{1/2} m_1^2 m_2^2}{r_p^{7/2}} f(e) \tag{2}$$

where $G$ is the Newton gravitational constant, $c$ is the speed of light, $r_p$ is the closest distance at encounter, which is the pericenter distance for an elliptical orbit, and $f(e)$ is a function of eccentricity $e$. By inserting $f(e) = 425\pi/(32\sqrt{2})$ when $e = 1$ into Eqs. (1) and (2), one obtains the cross section for binary formation

$$\sigma = 2\pi \left(\frac{85\pi}{6\sqrt{2}}\right)^{2/7} \frac{G^2(m_1+m_2)^{10/7}(m_1m_2)^{2/7}}{c^{10/7}v_{\rm rel}^{18/7}} \quad (3)$$

where $\sigma = \pi b_{\rm max}^2$ by definition, $b_{\rm max}$ is the maximum impact parameter. Meanwhile, the impact parameter $b$ is related to $r_p$ by

$$r_p = \frac{b^2 v_{\rm rel}^2}{2G(m_1+m_2)} \quad (4)$$

when $G(m_1 + m_2) \gg bv_{\rm rel}^2$, which is satisfied in this study.

Since we aim to investigate the scenario where primordial black holes are dark matter, we assume the number density of primordial black holes follows that of dark matter. Specifically, for a dark matter halo with virial mass $M_{\rm vir}$, we use the NFW density profile (Navarro et al. 1996) to model the mass density

$$\rho_{\rm NFW}(r) = \frac{\rho_c}{\frac{r}{r_c}\left(1+\frac{r}{r_c}\right)^2}, \quad (5)$$

where $r$ is the radial distance to the halo center, and $\rho_c$ and $r_c$ are the characteristic mass density and characteristic radius of the NFW profile, respectively.

The binary primordial black hole formation rate is given by Bird et al. (2016) as

$$\mathcal{R}(M_{\rm vir}) = 4\pi \int_0^{R_{\rm vir}} \frac{r^2}{2}\left(\frac{f_{\rm PBH}\rho_{\rm NFW}(r)}{M_{\rm PBH}}\right)^2 \langle\sigma v_{\rm rel}\rangle dr, \quad (6)$$

where $R_{\rm vir}$ is the halo virial radius, $f_{\rm PBH}$ is the mass fraction of primordial black holes in dark matter, the angle bracket is averaged with respect to the relative velocity distribution, which is modelled to be Maxwell-Boltzmann distribution

$$P(v_{\rm rel}) = N_0\left[\exp\left(-\frac{v_{\rm rel}^2}{v_{\rm max}^2}\right) - \exp\left(-\frac{v_{\rm vir}^2}{v_{\rm max}^2}\right)\right] \quad (7)$$

in which $v_{\rm vir}$ is the circular velocity at virial radius, $v_{\rm max}$ is the maximum circular velocity, $N_0$ is the normalization factor. As demonstrated by Bird et al. (2016), the merger happens shortly after the formation of a binary, therefore the formation rate Eq. (6) is identical to the event rate for coalescence of binary primordial black holes. Eq. (6) can be integrated analytically, the result is

$$\mathcal{R}(M_{\rm vir}) = \left(\frac{85\pi}{6\sqrt{2}}\right)^{2/7} \frac{2\pi G^2 f_{\rm PBH}^2 M_{\rm vir}^2 D(v_{\rm max})}{3cr_s^3 g^2(C)} \times \left[1 - \frac{1}{(1+C)^3}\right], \quad (8)$$

where $C = R_{\rm vir}/r_c$ is the concentration parameter for dark matter halo, $g(C) = \ln(1+C) - C/(1+C)$ and

$$D(v_{\rm rel}) = \int_0^{v_{\rm vir}} P(v_{\rm rel}; v_{\rm max})\left(\frac{2v}{c}\right)^{3/7} dv. \quad (9)$$

Finally, the overall event rate for binary primordial black hole coalescence is obtained by taking the sum of the contributions from all dark matter halos

$$\mathcal{R}_{\rm PBH} = \int \mathcal{R}(M_{\rm vir})\frac{dN}{dM_{\rm vir}} dM_{\rm vir} \quad (10)$$

We have made use of the python code `colossus` (Diemer 2018) to generate the dark matter halo mass function $dN/dM_{\rm vir}$ using the parametrized formula fitting to N-body simulation proposed by Tinker et al. (2008), and the concentration-dark matter halo mass relation proposed by Prada et al. (2012). We have tested systematics by using Raeymaekers (2007) from N-body simulation fits for dark matter halo mass function, and Dutton & Macciò (2014) for concentration-halo mass relation. Results show a different choice of dark matter halo population modeling will not change the final event rate by orders of magnitude.

Assuming $f_{\rm PBH} = 100\%$, the result of Eq. (10) is shown in Fig. 1. The main contribution to the integral in Eq. (10) is from low mass dark matter halos, therefore the result depends sensitively on the lower end for halo mass. To illustrate the dependence on lower mass cutoff $M_{\rm vir}^{\rm low}$, we plot $\mathcal{R}_{\rm PBH}$ as a function of $M_{\rm vir}^{\rm low}$ in Fig. 1. Also note that the integrand of Eq. (10) does not depend on $M_{\rm PBH}$ due to compensation between the primordial black hole number density and the cross section. To determine the lower limit of dark matter halo mass for $M_{\rm PBH} = 0.01/0.1/1\ M_\odot$, we follow the criterion by Eq. (11) of Bird et al. (2016) requiring that the dark matter halo evaporation time scale due to dynamical relaxation exceeds the dark energy domination time scale ($\sim 3\times10^9$ year). This choice results in the lower integral limit of Eq. (10) being $0.3/3/21\ M_\odot$ for $M_{\rm PBH} = 0.01/0.1/1\ M_\odot$. Choosing a lighter dark matter halo cutoff would contribute more binary primordial black hole merger events if the halos would not have evaporated at present and the NFW profile is still preserved. High resolution dark matter N-body simulations

are needed to precisely resolve the smallest structure of sub-solar mass primordial black hole halos but is beyond the scope of this paper.

With the above choices of lower integral cutoff, as shown in Fig. 1, the event rate for $M_{\rm PBH} = 0.01/0.1/1 M_\odot$ is 528/140/45 Gpc$^{-3}$ yr$^{-1}$. As a comparison, for $M_{\rm PBH} = 30 M_\odot$, the event rate is $\mathcal{O}(1)$ Gpc$^{-3}$ yr$^{-1}$ as computed in Bird et al. (2016). Therefore, the merger rate of sub-solar primordial black holes increases by one to two orders of magnitude compared to that of $30 M_\odot$.

To compare with observation, the sensitive volume, which is defined to be the orientation-averaged volume assuming a match-filtering signal-to-noise ratio (SNR) > 8 (Abbott et al. 2018b), is $\mathcal{O}(10^{-7})/\mathcal{O}(10^{-4})/\mathcal{O}(10^{-2})$ Gpc$^3$ for $M_{\rm PBH} = 0.01/0.1/1 M_\odot$ for Advanced LIGO at its design sensitivity. Given the above estimated event rate, under our assumption of delta function mass distribution, the second generation detectors are capable of detecting $M_{\rm PBH} = 1 M_\odot$ sources with $\mathcal{O}(1)$ year run, and would not be likely to observe $0.1 M_\odot$ and $0.01 M_\odot$ sources. Third generation detectors such as Cosmic Explorer (Reitze et al. 2019) and Einstein Telescope (Punturo et al. 2010) are expected improve the sensitive volume by three orders of magnitude compared to the second generation, thus it would be able to detect a delta function mass of $M_{\rm PBH} = 0.1 M_\odot$ source every $\mathcal{O}(0.1)$ year, and a $0.01 M_\odot$ source with $\mathcal{O}(10)$ year observation time. Conversely, a non-detection in the future would put constraints on the abundance of primordial black holes formed in this late Universe channel.

We also compare the binary coalescence rate to that derived from primordial black hole binary formation in the early Universe. Using the derivation by Sasaki et al. (2016), the merger rate is $\mathcal{O}(10^8)/\mathcal{O}(10^7)/\mathcal{O}(10^6)$ Gpc$^{-3}$ yr$^{-1}$ for $M_{\rm PBH} = 0.01/0.1/1\ M_\odot$ assuming $f_{\rm PBH} = 100\%$. Therefore, early Universe formation scenario dominates the event rate for sub-solar mass compact binary coalescence, but this formation channel is not expected to yield eccentric binaries because they would have been circularized in the local Universe. There are also model uncertainties under active investigation about what fraction of primordial black hole binaries would be disrupted after formation in the early Universe (Ali-Haïmoud et al. 2017; Raidal et al. 2019; Vaskonen & Veermäe 2020; Jedamzik 2020). If a significant fraction are disrupted, the merger rate for early Universe formation channel would be suppressed.

Compact binaries formed through dynamical interaction may retain eccentricity within the ground-based gravitational-wave detector frequency band. In the following we determine the eccentricity distribution for binary primordial black hole merger events following the references O'Leary et al. (2009); Cholis et al. (2016).

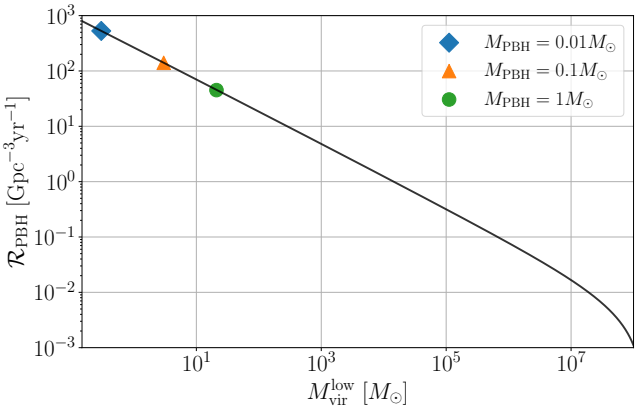


**Figure 1.** Event rate for binary primordial black hole merger as a function of the lower cut-off of dark matter halo mass. The markers are the event rate for $M_{\rm PBH} = 0.01/0.1/1 M_\odot$, which are 528/140/45 Gpc$^{-3}$ yr$^{-1}$, respectively.

Right after formation, the initial semi-major distance of a binary is given by

$$a_0 = \frac{G m_1 m_2}{2|E_f|} \tag{11}$$

where $E_f = 1/2 \mu v_{\rm rel}^2 - \delta E_{\rm GW}$. Combining Eqs. (4) and (11) and inserting the relation $r_{p,0} = a_0(1-e_0)$, one obtains an expression for the initial eccentricity at binary formation

$$e_0(m_1, m_2, v_{\rm rel}, b) = \sqrt{1 - \frac{2|E_f| b^2 v_{\rm rel}^2}{(m_1+m_2) m_1 m_2}} \tag{12}$$

After formation of the binary, the semi-major distance $a$ and the eccentricity $e$ gradually decay due to gravitational wave emission, the time evolution equation is given by (Peters 1964)

$$\begin{aligned} \frac{da}{dt} &= -\frac{64}{5} \frac{G^3 m_1 m_2 (m_1+m_2)}{c^5 a^3 (1-e^2)^{7/2}} \left(1 + \frac{73}{24} e^2 + \frac{37}{96} e^4\right), \\ \frac{de}{dt} &= -\frac{304}{15} \frac{G^3 m_1 m_2 (m_1+m_2) e}{c^5 a^4 (1-e^2)^{5/2}} \left(1 + \frac{121}{304} e^2\right). \end{aligned} \tag{13}$$

Combining Eq. (13) yields the expression for $da/de$ which can be integrated analytically, the result is

$$a(e) = a_0 \frac{\kappa(e)}{\kappa(e_0)} \tag{14}$$

where $\kappa(e)$ is a function of $e$

$$\kappa(e) = \frac{e^{12/19}}{1-e^2} \left(1 + \frac{121}{304} e^2\right)^{870/2299}. \tag{15}$$

Substituting Eqs. (11) and (12) and $a = \sqrt[3]{G(m_1+m_2)/\pi^2 f_{\rm GW}^2}$ from the Kepler third law where the frequency $f_{\rm GW} = 10$Hz, the non-linear Eq. (14) for $e^{10\rm Hz}$ can be solved by numerically finding the root.

As $e^{10\rm Hz}$ depends on $e_0$, which in turn depends on the initial relative velocity $v_{\rm rel}$ and the impact parameter $b$ for two black holes, we compute the relative velocity distribution by taking the derivative of $\mathcal{R}_{\rm PBH}$ with respect to $v_{\rm rel}$. The results are presented in Fig. 2. It can be seen that the initial relative velocity for $M_{\rm PBH} = 0.01/0.1/1\ M_\odot$ peak at 5/10/25 m/s, which approximately correspond to the typical velocity of the lightest dark matter halo in the integral Eq. (10), because the merger events from the low mass dark matter halo dominate the event rate.

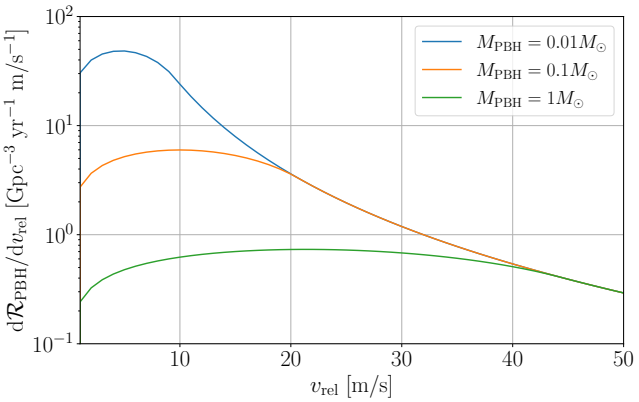


**Figure 2.** The binary primordial black hole event rate density with respect to the relative velocity $v_{\rm rel}$ at the formation of primordial black hole binaries for $M_{\rm PBH} = 0.01/0.1/1\ M_\odot$.

We use a Monte Carlo method to simulate a population of binary primordial black holes with mass $0.01/0.1/1 M_\odot$, respectively, each containing $\sim 10^6$ sources, to obtain the distribution of $e^{10\rm Hz}$. The square of the impact parameter, $b^2$, is chosen to be uniformly distributed in $[r_{\rm ISCO}^2, b_{\rm max}^2]$ (Cholis et al. 2016), where $r_{\rm ISCO}$ is the innermost stable circular orbit for Schwarzschild black hole (six times of Schwarzschild radius), $b_{\rm max}$ is given by Eq. (3). The initial relative velocity is drawn from the distribution in Fig. 2.

The results for the distribution of $e^{10\rm Hz}$ are shown in Fig. 3 by the step plots. To assist understanding, we also plot the cumulative probability distribution in Fig. 3 as shown by the solid lines converged to 100% at the right vertical axis. As seen from the figure, lighter primordial black holes tend to retain larger eccentricity. For $M_{\rm PBH} = 0.01/0.1/1\ M_\odot$, Up to 89%/40%/12% of the total inspiral events have $e^{10\rm Hz} \geq 0.01$, and up to 29%/9%/3% have $e^{10\rm Hz} \geq 0.1$. To connect these estimates with observation, assuming $f_{\rm PBH} = 100\%$, we find that second generation detectors would be expected to detect an eccentric binary coalescence with $M_{\rm PBH} = 1M_\odot$ with a few years observation time, while the third generations are expected to probe the eccentric events down to $0.01M_\odot$ with $10^3$ times of sensitive volume than advanced LIGO and Virgo. In addition, third generation detectors are designed increase sensitivity at frequencies of $\sim 2-5$ Hz, where the eccentricity will be more significant. Third generation detectors show promise to detect or constrain our understanding of eccentric binaries.

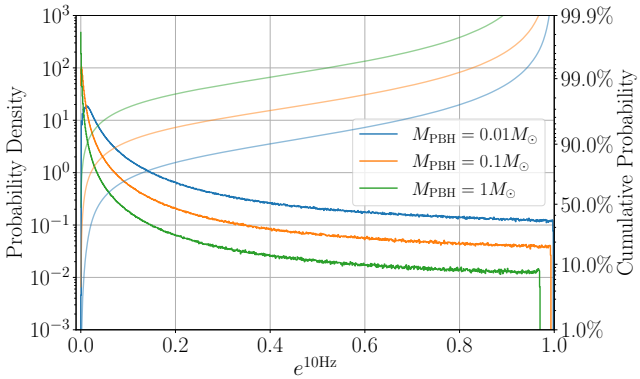


**Figure 3.** The probability density distribution (left y axis, step plots) and the cumulative probability density distribution (right y axis, straight lines) for the eccentricity of binary primordial black hole inspiral at gravitational wave frequency 10 Hz.

We further investigate the impact of $M_{\rm PBH}$ and $v_{\rm rel}$ on the eccentricity distribution. In Fig. 4, the mass $M_{\rm PBH}$ is fixed to 0.1 $M_\odot$, and the initial relative velocity $v_{\rm rel}$ is chosen to be 20/200/2000 m/s. The $e^{10\rm Hz}$ results show that higher relative velocity leads to the formation of more eccentric binaries. The cutoff for each distribution at the lowest eccentricity in Fig. 4 represents the binaries that would have been circularized the most at gravitational wave frequency 10 Hz and are from those with the widest separation at initial formation and thus the lowest initial eccentricity, as can be seen from Eq. (12).

The eccentricity distribution for fixed $v_{\rm rel}$ but different masses are in shown Fig. 5. The relative velocity is chosen to be 2 km/s, which is the typical velocity for $10^6\ M_\odot$ dark matter halos. The black hole mass is chosen to be $0.01/0.1/1/30\ M_\odot$. As considered by Cholis et al. (2016) and shown in Fig. 5, a majority of 30 $M_\odot$ binary black holes have eccentricity near 0 at 10 Hz. However, the sub-solar mass binaries all have non-zero peaks for eccentricity. In particular, for 0.01 $M_\odot$ primordial black holes in the $10^6\ M_\odot$ dark matter halos, all binaries have high eccentricity not lower than 0.7 at formation. Similarly, the lowest eccentricity cutoff for

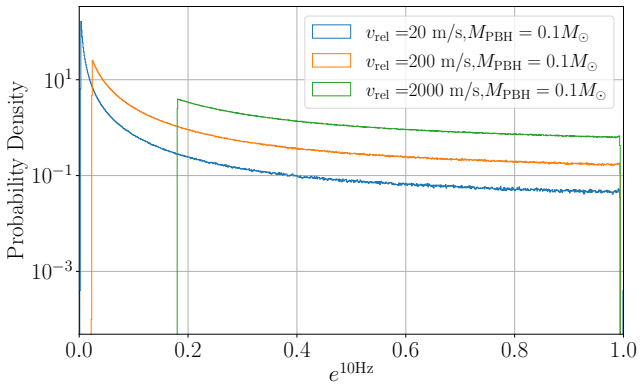


**Figure 4.** The eccentricity distribution at 10 Hz for primordial black hole binaries with $M_{\rm PBH} = 0.1\ M_\odot$ for three choices of relative velocity 20/200/2000 m/s.

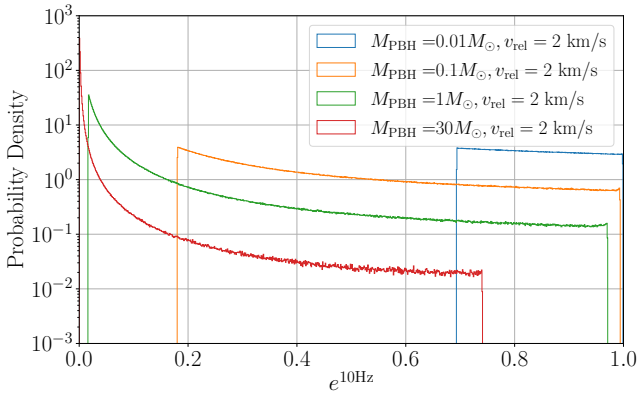


**Figure 5.** The eccentricity distribution at 10 Hz for primordial black hole binaries with $M_{\rm PBH} = 0.01/0.1/1/30 M_\odot$ with relative velocity fixed to 2 km/s.

each distribution represented the most circularized binaries in the simulated sources.

The above numerical results show that sub-solar mass compact binaries with high initial relative velocity tend to be more eccentric compared to the more massive binary black holes with low relative velocity. Therefore, the impact of eccentricity on targeted gravitational-wave searches for sub-solar mass compact binary coalescences deserves a more detailed study. We present our investigation in the next section.

## 3. IMPACT OF ECCENTRICITY ON GRAVITATIONAL-WAVE SEARCHES

There has been one search targeting gravitational waves from eccentric compact binary coalescence using model-based matched filtering (Nitz et al. 2020), where the authors searched for signals from eccentric binary neutron star mergers. The LIGO and Virgo Scientific Collaborations have also performed a non-modelled generic search for eccentric binary black hole mergers (Abbott et al. 2019). Most targeted searches for compact binary coalescence use quasi-circular orbit waveform template banks, including the direct searches for sub-solar mass black holes (Abbott et al. 2018a, 2019; Nitz & Wang 2021),

As demonstrated in section 2, sub-solar mass primordial black holes can retain non-zero eccentricity in the LIGO and Virgo frequency band if they form at the late Universe through dynamical capture. We aim to quantitatively study the potential loss in detection sensitivity when using only quasi-circular waveform template banks to search for signals from eccentric binary primordial black holes. To quantify the SNR of gravitational wave detection, we define the following noise-weighted inner product

$$(h_1, h_2) = 4\Re \int \frac{h_1(f) h_2^*(f)}{S_n(f)} \tag{16}$$

where $h_1$ and $h_2$ are signals or gravitational wave templates in the Fourier domain and $S_n(f)$ is the one-sided noise power spectral density. In this section we only consider the Advanced LIGO design sensitivity in the frequency range of $[20, 1024]$ Hz. The matched-filter SNR between the detector output $s$ and the template $h$ is defined to be

$$\rho = \frac{(s, h)}{\sqrt{(h, h)}}. \tag{17}$$

To measure the similarity between two waveform templates $h_1$ and $h_2$, the overlap function is defined as the normalized inner product

$$\mathcal{O}(h_1, h_2) = \frac{(h_1, h_2)}{\sqrt{(h_1, h_1)(h_2, h_2)}}. \tag{18}$$

Two templates may be different up to a constant time and phase in the Fourier domain, thus the match function between two waveforms is given by maximizing over the offset of coalescence time $t_c$ and an overall phase $\phi_c$

$$\mathcal{M}(h_1, h_2) = \max_{t_c, \phi_c} \left( \mathcal{O}(h_1, h_2 e^{i(2\pi f t_c - \phi_c)}) \right). \tag{19}$$

There have been several waveform approximants modeling eccentric compact binary coalescence, such as Moore et al. (2016); Huerta et al. (2018); Liu et al. (2020); Chiaramello & Nagar (2020). In this work, we utilize the model proposed by Moore & Yunes (2019a,b); Moore et al. (2018), referred to as `TaylorF2e` [1], for speedy waveform generation. `TaylorF2e` is an inspiral waveform developed in the Fourier domain and is

[1] The source code can be found in https://github.com/gwastro/TaylorF2e

accurate to the third post-Newtonian order. The eccentricity is valid up to at least 0.8 in the low mass case $\sim 1M_\odot$ (Moore & Yunes 2019b), which is sufficient for our purpose to investigate the eccentricity of sub-solar mass compact binaries.

In order to extract gravitational-wave signals in the data, a targeted search (Usman et al. 2016; Messick et al. 2017) builds a pre-calculated template bank to match filter the data. To measure the detection ability of a template bank built with quasi-circular waveforms to search for eccentric binaries, we first generate a template bank by a geometric method based on hexagonal lattice placement (Cokelaer 2007; Brown et al. 2012) using the quasi-circular waveform approximant `TaylorF2` (Buonanno et al. 2009). For this study, we assume the component black holes will have negligible spin. The template bank is designed to recover sources with component masses in the range $[0.1, 1]\ M_\odot$. The bank is discrete in the parameter space, and we require the maximum mismatch due to discreteness is no higher than 3% by construction. The above setting results in a bank with 6995517 templates.

Next we generate simulated gravitational-wave data with a source population using the `TaylorF2e` approximant. The mock data are then compared with every template in the bank using Eq. (19) to obtain the maximum match "fitting factor" over the entire template bank. A fitting factor of $x$ would lead to $1 - x^3$ loss of the detection rate for a search with a fixed amount of noise, as the gravitational-wave search SNR would be decreased to $x$ times the theoretically optimal value.

In Fig. 6, we generate eccentric sub-solar mass binary black hole gravitational wave signals and compute the fitting factor with respect to the non-eccentric template bank. Each point in the figure represents a mock signal injection.

In the left panel of Fig. 6, the binaries are chosen to have equal mass. $M_{\rm PBH}$ and $e^{10\rm Hz}$ are uniformly distributed in $[0.1, 1]\ M_\odot$ and $[0, 0.2]$, respectively. The fitting factor for $e^{10\rm Hz}$ and the chirp mass $M_{\rm chirp} = (m_1 m_2)^{3/5}(m_1 + m_2)^{1/5}$ ($\sim 0.87 M_{\rm PBH}$ for equal mass) is presented. The figure also illustrates the 97% and 80% contour lines obtained from fitting the plot. The figure shows the trend that the fitting factor gets worse for higher eccentricity, and also for lighter binaries because of their longer duration. For component mass $m = 0.1/1 M_\odot$, the fitting factor drops below 97% with $e^{10\rm Hz} \geq 0.003/0.20$.

In the right panel of Fig. 6, we consider the impact on fitting factor from different mass ratios by fixing $M_{\rm chirp} = 0.4\ M_\odot$. The mass ratio is uniformly distributed in $[1, 4]$ and the eccentricity is uniformly in $[0, 0.2]$. As shown, the 97% and 80% fitting factor lines only depend weakly on the mass ratio and decrease for higher mass ratio.

We also consider more realistic distributions for $e^{10\rm Hz}$ as derived in Fig. 3 of Section 2. We generate two groups of mock data each with $\sim 2000$ signals using `TaylorF2e`. The component mass is $0.1 M_\odot$ and $1 M_\odot$, respectively, and only equal mass binaries are considered. The inclination angle is chosen to be uniformly distributed in $[-\pi/2, \pi/2]$, the polarization angle is uniformly in $[0, 2\pi]$, the source sky location is isotropic. The eccentricity distribution are drawn from Fig. 3 for $0.1 M_\odot$ and $1 M_\odot$ sources accordingly.

The cumulative probability with respect to the fitting factor is shown in Fig. 7. The vertical dashed line in Fig. 7 denotes 97%, which all the signals with zero eccentricity should exceed by construction of the template bank . However, due to the existence of eccentricity, for $M_{\rm PBH} = 0.1 M_\odot$, up to 68% of the signals have fitting factor lower than 97%, and 41% have fitting factor lower than 80%. For $M_{\rm PBH} = 1\ M_\odot$, 15% signals have fitting factor lower than 97%, and 6% signals have fitting factor lower than 80%. Also note that, when fitting factor is low, the mismatch between signals and templates may be significant enough to cause issues with signal-based vetoes (Allen 2005) which would further reduce the detection rate of eccentric sources. Therefore our results based on fitting factor are a conservation estimation for the loss of detection rate.

Given that fitting factor can only measure the fractional recovered SNR for a single injected signal, we use the effective fitting factor $FF_{\rm eff}$ (Harry et al. 2016, 2014; Buonanno et al. 2003) to account for the overall fraction for detection loss for a whole group of simulated signals. The effective fitting factor is defined as a mean average of fitting factors weighted by the signal amplitude

$$FF_{\rm eff} = \left( \frac{\sum_{i=1}^{N} FF_i^3 \sigma_i^3}{\sum_{i=1}^{N} \sigma_i^3} \right)^{1/3}, \qquad (20)$$

where the subscript $i$ denotes the i-th mock injection, $N$ is the total number of signals, $FF_i$ is the fitting factor, $\sigma_i = \sqrt{(h_i|h_i)}$ is the optimal SNR for the i-th signal. An effective fitting factor of $x$ would lead to $1 - x^3$ loss of detection rate.

For our two groups of injection with $M_{\rm PBH} = 0.1\ M_\odot$ and $1 M_\odot$, $FF_{\rm eff} = 83\%$ and 95.8%, respectively, which corresponds to an overall loss of 42% and 12% of signals compared to the idealized maximum. For comparison, if only selecting the injected signals with $e^{10\rm Hz} = 0$, the effective fitting factor is 99.7% for $M_{\rm PBH} = 0.1 M_\odot$ and 97.8% for $M_{\rm PBH} = 1 M_\odot$, which corresponds to 0.9% and 6.4% loss, which arises from the discreteness of tem-

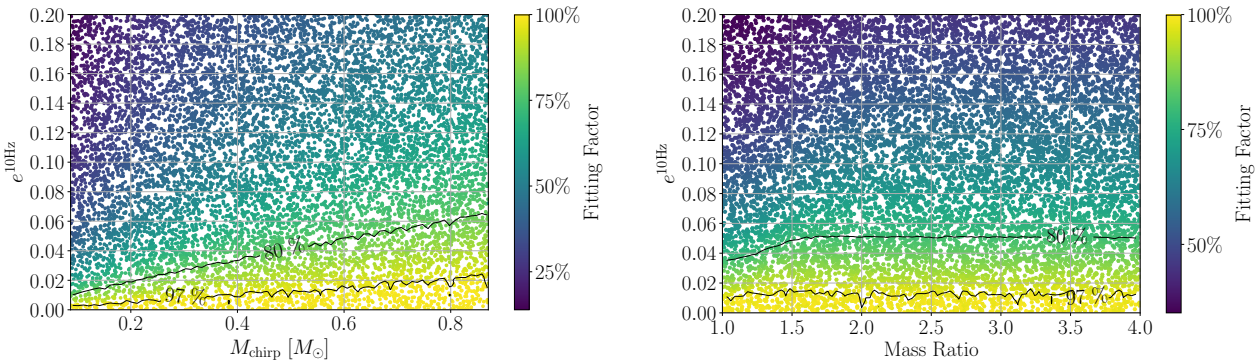


**Figure 6.** The fitting factor for simulated data of eccentric sub-solar binary black hole coalescences with respect to the template bank constructed from a quasi-circular waveform approximant. Each point represents an injected mock signal. In the left panel, the signals are generated from equal mass binaries with component mass in [0.1.1] $M_\odot$ uniformly. In the right panel, the chirp mass is fixed to 0.4 $M_\odot$ and the mass ratio is in $[1, 4]$.

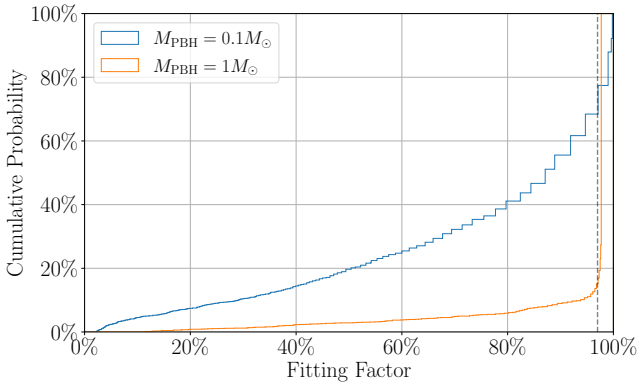


**Figure 7.** Cumulative distribution for fitting factor for gravitational wave sources with $0.1M_\odot$ and $1M_\odot$ and eccentricity distributions derived from Section 2. The vertical dash line denotes 97%, which represents the lower limit for fitting factor for signals without eccentricity.

plate bank. After subtracting the signals missed due to template bank discreteness, for $M_{\mathrm{PBH}} = 0.1M_\odot$ and $M_{\mathrm{PBH}} = 1\ M_\odot$ sources within the late Universe dynamical encounter model, we conclude that the eccentricity effects can lead to loss of 41% and 6% of the signals, respectively, by targeted search with a quasi-circular waveform template bank using Advanced LIGO at its designed sensitivity. For primordial black holes with an extended mass in the range $[0.1, 1]M_\odot$, we expect the the corresponding results for loss of detection should lie in between.

## 4. DISCUSSIONS AND CONCLUSIONS

In this work, we investigate the prospects for detecting gravitational wave signals from eccentric sub-solar mass binary black hole inspiral, which would be a signature for primordial black hole binaries formed by dynamical capture in the local Universe. The merger rate and eccentricity distribution for binaries assuming a delta function mass distribution varying in $[0.01, 1]M_\odot$ are derived. For $1M_\odot - 1\ M_\odot$ binaries, the detection rate is $\mathcal{O}(1)$/year for Advanced LIGO and Virgo with design sensitivity, if primordial black holes account for a majority of dark matter, and 12%(3%) of the sources have $e^{10\mathrm{Hz}} \geq 0.01(0.1)$, thus eccentric signals may be detected with a few years of observation based on the assumed model. For $0.1 - 0.1M_\odot$ and $0.01 - 0.01\ M_\odot$ binaries the detection rate would be too low for the second generation ground-based detectors, but is promising to be detected by the third generation detectors. Conversely, non-detection in the future would put constraints on our understanding for this formation channel.

We also investigate what fraction of the eccentric binaries can be missed by using quasi-circular waveform template bank. Results show current targeted searches can miss 41% and 6% of the events with component mass $0.1M_\odot$ and $1M_\odot$, respectively, with Advanced LIGO designed sensitivity, due to the eccentricity of primordial black hole binaries arising from dynamical encounter in the local Universe.

For the formation scenario of primordial black hole binaries, we only consider the two-body direct capture through gravitational-wave braking. Other mechanisms such as three body interaction via Kozai-Lidov effects (Kozai 1962; Lidov 1962) may further improve the event rate, and would be interesting to consider in a future work.

The third generation gravitational wave detectors such as Cosmic Explorer (Reitze et al. 2019) and Einstein Telescope (Punturo et al. 2010) are being planned. The detection volume is expected to increase three orders of magnitude compared to the second generation. Moreover, the sensitive band can be pushed down to $\sim$ 2 Hz, at which the eccentricity for primordial black

hole binaries is more significant than later at 10 Hz as considered in this work. Third generation detectors are even more promising to hunt for eccentric gravitational waves signals.

## ACKNOWLEDGMENTS

We acknowledge the Max Planck Gesellschaft for support and the Atlas cluster computing team at AEI Hannover.

## REFERENCES


Aasi, J., et al. 2015, Class. Quantum Grav., 32, 074001, doi: 10.1088/0264-9381/32/7/074001

Abbott, B., et al. 2019, Astrophys. J., 883, 149, doi: 10.3847/1538-4357/ab3c2d

Abbott, B. P., Abbott, R., Abbott, T. D., et al. 2016a, ApJL, 833, L1, doi: 10.3847/2041-8205/833/1/L1

—. 2016b, ApJS, 227, 14, doi: 10.3847/0067-0049/227/2/14

—. 2017, Nature, 551, 85, doi: 10.1038/nature24471

—. 2018a, PhRvL, 121, 231103, doi: 10.1103/PhysRevLett.121.231103

—. 2018b, Living Reviews in Relativity, 21, 3, doi: 10.1007/s41114-018-0012-9

—. 2019, PhRvD, 100, 024017, doi: 10.1103/PhysRevD.100.024017

Abbott, R., Abbott, T. D., Abraham, S., et al. 2020, arXiv e-prints, arXiv:2010.14527. https://arxiv.org/abs/2010.14527

Acernese, F., et al. 2015, Class. Quantum Grav., 32, 024001, doi: 10.1088/0264-9381/32/2/024001

Ali-Haïmoud, Y., Kovetz, E. D., & Kamionkowski, M. 2017, PhRvD, 96, 123523, doi: 10.1103/PhysRevD.96.123523

Allen, B. 2005, Phys. Rev. D, 71, 062001, doi: 10.1103/PhysRevD.71.062001

Bird, S., Cholis, I., Muñoz, J. B., et al. 2016, PhRvL, 116, 201301, doi: 10.1103/PhysRevLett.116.201301

Brown, D. A., Harry, I., Lundgren, A., & Nitz, A. H. 2012, Phys. Rev. D, 86, 084017, doi: 10.1103/PhysRevD.86.084017

Buonanno, A., Chen, Y.-b., & Vallisneri, M. 2003, Phys. Rev. D, 67, 104025, doi: 10.1103/PhysRevD.67.104025

Buonanno, A., Iyer, B. R., Ochsner, E., Pan, Y., & Sathyaprakash, B. S. 2009, PhRvD, 80, 084043, doi: 10.1103/PhysRevD.80.084043

Byrnes, C. T., Hindmarsh, M., Young, S., & Hawkins, M. R. S. 2018, JCAP, 08, 041, doi: 10.1088/1475-7516/2018/08/041

Carr, B., Clesse, S., García-Bellido, J., & Kühnel, F. 2021, Phys. Dark Univ., 31, 100755, doi: 10.1016/j.dark.2020.100755

Carr, B., & Kuhnel, F. 2020, Ann. Rev. Nucl. Part. Sci., 70, 355, doi: 10.1146/annurev-nucl-050520-125911

Carr, B. J., & Hawking, S. W. 1974, MNRAS, 168, 399, doi: 10.1093/mnras/168.2.399

Chiaramello, D., & Nagar, A. 2020, PhRvD, 101, 101501, doi: 10.1103/PhysRevD.101.101501

Cholis, I., Kovetz, E. D., Ali-Haïmoud, Y., et al. 2016, PhRvD, 94, 084013, doi: 10.1103/PhysRevD.94.084013

Cokelaer, T. 2007, PhRvD, 76, 102004, doi: 10.1103/PhysRevD.76.102004

Diemer, B. 2018, ApJS, 239, 35, doi: 10.3847/1538-4365/aaee8c

Dutton, A. A., & Macciò, A. V. 2014, MNRAS, 441, 3359, doi: 10.1093/mnras/stu742

Green, A. M., & Kavanagh, B. J. 2020, arXiv e-prints, arXiv:2007.10722. https://arxiv.org/abs/2007.10722

Harry, I., Privitera, S., Bohé, A., & Buonanno, A. 2016, PhRvD, 94, 024012, doi: 10.1103/PhysRevD.94.024012

Harry, I. W., Nitz, A. H., Brown, D. A., et al. 2014, PhRvD, 89, 024010, doi: 10.1103/PhysRevD.89.024010

Hawking, S. 1971, MNRAS, 152, 75, doi: 10.1093/mnras/152.1.75

Huerta, E. A., Moore, C. J., Kumar, P., et al. 2018, PhRvD, 97, 024031, doi: 10.1103/PhysRevD.97.024031

Jedamzik, K. 1997, Phys. Rev. D, 55, 5871, doi: 10.1103/PhysRevD.55.R5871

—. 2020. https://arxiv.org/abs/2007.03565

Kozai, Y. 1962, AJ, 67, 591, doi: 10.1086/108790

Lidov, M. L. 1962, Planet. Space Sci., 9, 719, doi: 10.1016/0032-0633(62)90129-0

Liu, X., Cao, Z., & Shao, L. 2020, PhRvD, 101, 044049, doi: 10.1103/PhysRevD.101.044049

Maggiore, M. 2008, Gravitational Waves: Volume 1: Theory and Experiments, Gravitational Waves (OUP Oxford). https://books.google.de/books?id=AqVpQgAACAAJ

Messick, C., Blackburn, K., Brady, P., et al. 2017, PhRvD, 95, 042001, doi: 10.1103/PhysRevD.95.042001

Moore, B., Favata, M., Arun, K. G., & Mishra, C. K. 2016, PhRvD, 93, 124061, doi: 10.1103/PhysRevD.93.124061

Moore, B., Robson, T., Loutrel, N., & Yunes, N. 2018, Classical and Quantum Gravity, 35, 235006, doi: 10.1088/1361-6382/aaea00

Moore, B., & Yunes, N. 2019a, Classical and Quantum Gravity, 36, 185003, doi: 10.1088/1361-6382/ab3778

—. 2019b, arXiv e-prints, arXiv:1910.01680. https://arxiv.org/abs/1910.01680

Nakamura, T., Sasaki, M., Tanaka, T., & Thorne, K. S. 1997, ApJL, 487, L139, doi: 10.1086/310886

Navarro, J. F., Frenk, C. S., & White, S. D. M. 1996, ApJ, 462, 563, doi: 10.1086/177173

Nitz, A. H., Lenon, A., & Brown, D. A. 2020, ApJ, 890, 1, doi: 10.3847/1538-4357/ab6611

Nitz, A. H., & Wang, Y.-F. 2021, Phys. Rev. Lett., 126, 021103, doi: 10.1103/PhysRevLett.126.021103

Nitz, A. H., Dent, T., Davies, G. S., et al. 2019, Astrophys. J., 891, 123, doi: 10.3847/1538-4357/ab733f

O'Leary, R. M., Kocsis, B., & Loeb, A. 2009, MNRAS, 395, 2127, doi: 10.1111/j.1365-2966.2009.14653.x

Peters, P. C. 1964, Physical Review, 136, 1224, doi: 10.1103/PhysRev.136.B1224

Peters, P. C., & Mathews, J. 1963, Physical Review, 131, 435, doi: 10.1103/PhysRev.131.435

Prada, F., Klypin, A. A., Cuesta, A. J., Betancort-Rijo, J. E., & Primack, J. 2012, MNRAS, 423, 3018, doi: 10.1111/j.1365-2966.2012.21007.x

Punturo, M., Abernathy, M., Acernese, F., et al. 2010, Classical and Quantum Gravity, 27, 194002, doi: 10.1088/0264-9381/27/19/194002

Raeymaekers, J. 2007, Fortschritte der Physik, 55, 811, doi: 10.1002/prop.200610362

Raidal, M., Spethmann, C., Vaskonen, V., & Veermäe, H. 2019, JCAP, 02, 018, doi: 10.1088/1475-7516/2019/02/018

Reitze, D., Adhikari, R. X., Ballmer, S., et al. 2019, in Bulletin of the American Astronomical Society, Vol. 51, 35. https://arxiv.org/abs/1907.04833

Sasaki, M., Suyama, T., Tanaka, T., & Yokoyama, S. 2016, PhRvL, 117, 061101, doi: 10.1103/PhysRevLett.117.061101

Suwa, Y., Yoshida, T., Shibata, M., Umeda, H., & Takahashi, K. 2018, MNRAS, 481, 3305, doi: 10.1093/mnras/sty2460

The LIGO Scientific Collaboration, the Virgo Collaboration, Abbott, R., et al. 2020a, arXiv e-prints, arXiv:2010.14533. https://arxiv.org/abs/2010.14533

—. 2020b, arXiv e-prints, arXiv:2010.14529. https://arxiv.org/abs/2010.14529

Timmes, F. X., Woosley, S. E., & Weaver, T. A. 1996, ApJ, 457, 834, doi: 10.1086/176778

Tinker, J., Kravtsov, A. V., Klypin, A., et al. 2008, ApJ, 688, 709, doi: 10.1086/591439

Turner, M. 1977, ApJ, 216, 610, doi: 10.1086/155501

Usman, S. A., Nitz, A. H., Harry, I. W., et al. 2016, Classical and Quantum Gravity, 33, 215004, doi: 10.1088/0264-9381/33/21/215004

Vaskonen, V., & Veermäe, H. 2020, Phys. Rev. D, 101, 043015, doi: 10.1103/PhysRevD.101.043015

Zel'dovich, Y. B., & Novikov, I. D. 1967, Soviet Ast., 10, 602